



---

## **Using High-Resolution Remote Sensing to Characterize Suspended Particulate Organic Matter as Bivalve Food for Aquaculture Site Selection**

Authors: Newell, Carter R., Hawkins, Anthony J. S., Morris, Kevin, Boss, Emmanuel, Thomas, Andrew C., et al.

Source: Journal of Shellfish Research, 40(1) : 113-118

Published By: National Shellfisheries Association

URL: <https://doi.org/10.2983/035.040.0110>

## USING HIGH-RESOLUTION REMOTE SENSING TO CHARACTERIZE SUSPENDED PARTICULATE ORGANIC MATTER AS BIVALVE FOOD FOR AQUACULTURE SITE SELECTION

CARTER R. NEWELL,<sup>1\*</sup> ANTHONY J. S. HAWKINS,<sup>2</sup> KEVIN MORRIS,<sup>3</sup> EMMANUEL BOSS,<sup>4</sup> ANDREW C. THOMAS,<sup>4</sup> THOMAS J. KIFFNEY<sup>5</sup> AND DAMIAN C. BRADY<sup>4</sup>

<sup>1</sup>Maine Shellfish R+D, 36 Pond Street, Bucksport, ME, 04416; <sup>2</sup>Plymouth Marine Laboratory, Prospect Place, The Hoe, Plymouth, United Kingdom, PL13DH; <sup>3</sup>Discovery Software, 11 St. Mary's Park, Paignton, Devon, United Kingdom, TQ47DA; <sup>4</sup>School of Marine Sciences, 360 Aubert Hall, University of Maine, Orono, ME 04469; <sup>5</sup>School of Marine Sciences, 193 Clarks Cove Road, University of Maine, Walpole, ME 04573

**ABSTRACT** Characterizing relative temporal and spatial variations in both the living and detrital components of bivalve food is required to predict bivalve growth across environments with contrasting seston compositions. The present article describes how remote sensing can be applied for such characterization, both over large spatial scales and fine spatial resolutions (i.e., farm scale; 10's of meters), thereby providing key information for bivalve aquaculture operations and site selection, including the restoration of native species. Using natural seawater samples collected from contrasting culture sites in North America and Europe, a simple model was developed to predict the total particulate organic matter (POM) available as food to bivalves from high-resolution remote-sensing images of coastal embayments which estimate chlorophyll (CHL) and turbidity, in which CHL acts as a proxy for living organics and turbidity as a measure of total suspended particulate matter (SPM). The resulting POM derived from satellite images, along with temperature and CHL, are then used as inputs to the bivalve bioenergetic model, ShellSIM, to predict the growth of *Mytilus edulis*, *Crassostrea virginica*, and *Ostrea edulis* along the coast of Maine, one of the most convoluted coasts in the United States, for aquaculture site selection.

**KEY WORDS:** remote sensing, bivalve food, aquaculture site selection, particulate organic matter, turbidity

### INTRODUCTION

Modeling bivalve filter feeder growth in response to environmental variables in the coastal zone has applications to coastal zone management, and may include determination of estuary-wide carrying capacity, site selection, and production capacity for aquaculture. The use of relatively new, high-resolution, remote-sensing data as input to bivalve growth models has been hampered by the lack of a method to estimate nonliving organics within the detrital elements of suspended matter, which may contribute substantially to growth (Hawkins et al. 2013a, 2013b). Thomas et al. (2011) used estimates of temperature and chlorophyll (CHL) from satellite data and a dynamic energy budget model to model mussel growth in the Mont Saint-Michel Bay, France, but the detrital components of food were not estimated. Furthermore, Snyder et al. (2017) used a growth index to map oyster growth based on temperature, CHL, and turbidity derived from Landsat 8 measurements along the Maine Coast, and Radiarta et al. (2008) applied a multicriteria evaluation approach using remote-sensing data for scallop aquaculture site selection in Japan; neither of these studies modeled growth itself.

Satellite remote sensing can provide routine information on temperature, CHL, turbidity, and colored dissolved organic matter over large areas of coast (Franz et al. 2015), but it does not estimate particulate organic matter (POM) directly. At the very highest turbidities, dilution of nutritious particles with inorganic sediments which are nondigestible may ultimately

limit bivalve growth. For example, Adams et al. (2019) found that the American oyster growth rate was a positive function of the CHL/turbidity ratio. Meanwhile, in less turbid estuaries, turbidity can be a useful indication of primary production involving phytoplankton and bioavailable phytodetritus, which provides enzyme hydrolyzable amino acids for bivalve nutrition during algal decay (Adams et al. 2019). Chlorophyll, an estimate of living phytoplankton biomass, has been related to particulate organic carbon, POC, in the euphotic zone (Legendre & Michaud 1999). Using optical and filtered samples following a diatom bloom in Japan, Wang et al. (2011) found that POC was also correlated with both SPM and CHL. Whereas *CHL-a* (CHL) is widely used as a proxy for the living organics available as food to bivalve shellfish, and which can work well in oligotrophic to hypereutrophic waters that are dominated by phytoplankton, there is a need to characterize nonliving detrital organics, which are also a main source of food to bivalves, from remote-sensing data. Wozniak et al. (2016) found a strong correlation among water surface reflectance or reflectance ratios and concentrations of SPM and POM in the Baltic Sea during four cruises in the spring and fall. However, no previous studies have related POM, which is used in bivalve growth models to include the detrital components of food, both to field CHL and turbidity (which is measured optically as a proxy for total suspended matter), which can be estimated from remote-sensing images in the coastal zone. The purpose of this article is to present an equation which can be used to predict POM, which in combination with CHL can then be used to estimate the living and nonliving food for bivalves from satellite images. Together with temperature, this allows the prediction of shellfish growth across contrasting environments as described

\*Corresponding author. E-mail: musselsandoysters@gmail.com  
DOI: 10.2983/035.040.0110

for ShellSIM (Hawkins et al. 2013a). Results are presented within the ShellGIS platform (Newell et al. 2013), as a tool toward optimizing aquaculture and restoration.

## MATERIALS AND METHODS

### Satellite Data

Conversion of the Landsat 8 IR channel data to sea surface temperature (SST) values followed the procedure presented by Thomas et al. (2002). In brief, each Landsat 8 daily IR data field is regressed against fully calibrated and atmospherically corrected NOAA Advanced Very High Resolution Radiometer SST data from the same day and location offshore. The Landsat 8 data are downscaled to the spatial resolution of Advanced Very High Resolution Radiometer data over their coincident coastal regions. An iterative regression approach that eliminates the most obvious atmospherically contaminated pixels converges on regression coefficients that relate the Landsat 8 channel values to SST. These values are then applied to the entire, full spatial resolution, Landsat 8 IR field, assuming a locally homogenous atmosphere.

Processing of Landsat 8 color channels followed the procedure outlined in Snyder et al. (2017). In brief, for mostly cloud-free days, top-of-the-atmosphere radiance was corrected for atmospheric inputs by finding a strongly absorbing, and thus very dark, humic lake within the scene and assuming all the blue signal emanating from it is due to the atmosphere. The appropriate atmospheric model was then removed from the full scene, and the reflectance at non-cloudy pixels was computed using NASA's SeaDAS environment. SPM and CHL were inverted from reflectance based on the reflectance at 665 nm and a reflectance ratio algorithm, respectively (Snyder et al. 2017).

### Prediction of Particulate Organic Matter from Landsat 8–Derived SPM and CHL

To assess whether POM might be predicted from SPM and/or CHL, measures from natural seawater samples collected in shellfish-growing areas in Maine and Connecticut (the Damariscotta River, ME and Branford, Long Island Sound) in 2010, 2011, and 2016 were collated together with similar measures from 12 other locations in Europe (Hawkins et al. 2013a), filtered on GFF filters and analyzed for SPM, POM, and CHL as described by Hawkins et al. (2013b). In total, these included 290 coincident samples for each variable, measured across wide ranges of CHL and SPM of up to 28  $\mu\text{g L}^{-1}$  and 210  $\text{mg L}^{-1}$ , respectively. Stepwise linear regression was then used to analyze the dependencies of POM on both CHL and SPM within all data combined.

### ShellGIS

The relative growth of individuals in three species, that is, *Crassostrea virginica*, *Mytilus edulis*, and *Ostrea edulis*, were presented in the desktop application ShellGIS (Newell et al. 2013) (<https://www.shellgis.com>), using satellite data from one date with the assumption that conditions were constant over a 30-day period.

Satellite products derived from Landsat 8 data for SST, CHL, and turbidity (SPM) as described earlier were provided in GeoTIFF format at 30, 60, and 60 m resolution, respectively.

Cloud-free satellite scenes obtained for Midcoast Maine for July 14, 2013, and for the Penobscot River area using data from August 23, 2016 were used to generate ShellGIS outputs.

Sea surface temperature and CHL were used as direct inputs into the ShellSIM model. Particulate organic matter was derived from the satellite data using the formula:  $\text{POM} = (0.153 \times \text{CHL}) + (0.194 \times \text{SPM})$  as described in Eq. 1 in the following text. Particulate organic matter images were calculated using raster tools in QGIS (Development Team Q.G.I.S. 2012).

To run ShellGIS, QGIS was used to clip the study area to Midcoast Maine and create a series of  $256 \times 256$  tiles covering the entire area. This required 84 tiles in the coastal zone, arranged  $12 \times 7$  zonally by meridian. Images were converted into ESRI float format images for import into ShellGIS, and then, .csv files were created for the loading of these data.

A number of coding modifications were made to ShellGIS to enable the import of the satellite data and to facilitate the use of constant values for the remaining model input data. The default values used for the other parameters were as follows: salinity: 30, aerial exposure: 0, current speed: 25  $\text{cm s}^{-1}$ , and dissolved oxygen: 8  $\text{mg L}^{-1}$ . Additional code was written to process each tile at a time, providing constant values for CHL and turbidity, and then used to predict drivers describing food availability as required by ShellSIM.

## RESULTS

### Prediction of Particulate Organic Matter from Landsat 8–Derived SPM and CHL

Analyzing the combined data from samples of natural seawater collected at 14 locations in both the United States and Europe, stepwise linear regression established highly significant separate dependencies of POM (mg/L) on both CHL ( $\mu\text{g/L}$ ) and SPM (mg/L) as follows:

$$\text{POM} = [0.153 (\pm 0.030) \times \text{CHL}] + [0.194 (\pm 0.008) \times \text{SPM}], \quad (1)$$

where  $\pm 2$  SE are bracketed for each parameter,  $r^2 = 0.94$ , residual  $df = 288$ , and  $P < 0.0001$ . To check whether Eq. 1 might be used to predict POM from Landsat 8–derived CHL and SPM, POM was predicted from all CHL and SPM illustrated in Figure 1 as  $\text{POMPRED (mg/L)} = (0.153 \times \text{CHL}) + (0.194 \times \text{SPM})$ . The linear regression where  $\text{POMPRED} = 0.939 (\pm 0.028) \times \text{POM}$ ,  $r^2 = 0.94$ , residual  $df = 289$ , and  $P < 0.0001$  established that 94% of the variance in POMPRED was predicted on the basis of CHL and SPM.

To check whether ShellSIM might use POMPRED derived as described earlier, and thus by inference Landsat 8–derived CHL and SPM, the aforementioned approach was applied using coincident measures of environmental drivers and oyster growth collected independently in both Maine and Connecticut during 2011. ShellSIM was calibrated for *Crassostrea virginica* from explicit measures of feeding behavior, together with literature values for responses to temperature, salinity, and other variables. Applying the single resulting set of parameters for this species within ShellSIM's standard set of functional interrelations, growth measured independently of water samples was simulated to less than 5% error across full ranges of environment variability and throughout normal culture practice in both the Damariscotta River and Long Island Sound (Fig. 2). In the

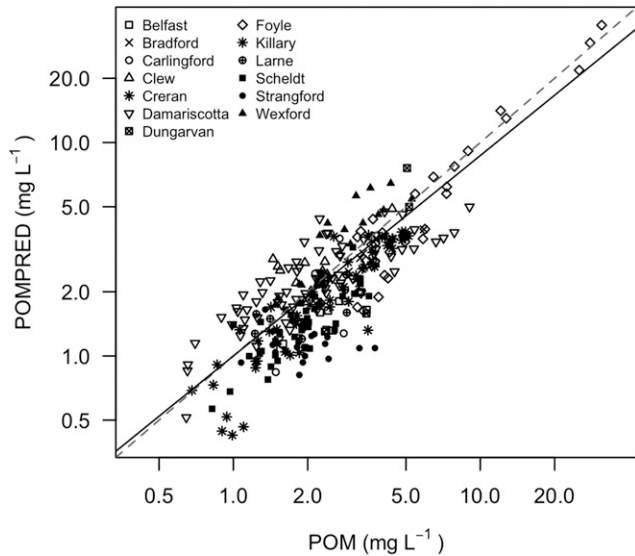


**Figure 1.** Relationship between the particulate organic matter (POM) predicted from measures of chlorophyll and SPM (POMPRED,  $\text{mg L}^{-1}$ ) and actual POM ( $\text{POM}$ ,  $\text{mg L}^{-1}$ ) measured in the same seawater samples from Damariscotta, ME, and Branford, CT, plus 12 other locations in Europe as described by Hawkins et al. (2013a). The dashed line is 1:1, and the black line is the regression (Eq. 1).

present study, POMPRED has been derived from the same measures of CHL and SPM as were used to drive those growth simulations, which have been rerun using POMPRED in place of actual measures of POM, maintaining all other drivers unchanged. Resulting growth simulations are also illustrated in Figure 2, showing how, for exactly the same ShellSIM parameter set, growth predicted on the basis of POMPRED was within 5% of that predicted using POM.

### ShellGIS

For the Midcoast Maine area, ShellGIS was run using five input dates from July to October to estimate bivalve growth.

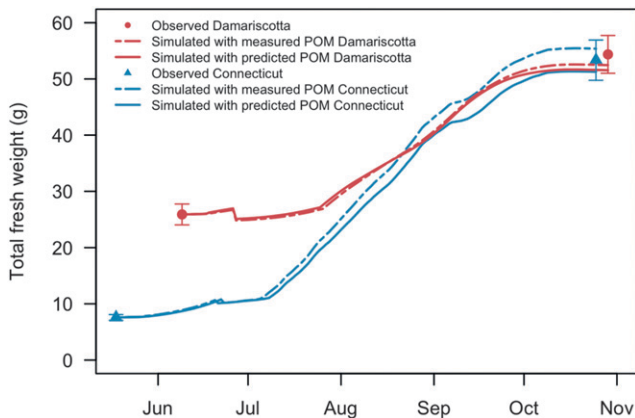


**Figure 2.** Comparisons of *Crassostrea virginica* growth simulated by ShellSIM with growth observed (mean  $\pm$  2 SE) throughout normal culture practiced in both the Damariscotta River, ME, and Long Island Sound, CT, and growth predicted using particulate organic matter derived by Eq. 1.

However, in many areas, cloud cover made it difficult to get a complete time series for each pixel over the whole region, so just one cloud-free date (July 14, 2013) was chosen. Consequently, the ShellGIS code was modified to allow the raster data to stay constant for the length of a shellfish growth model run for 30 days, allowing shellfish to grow measurably during that period. ShellSIM was run using data from the first date, July 14, 2013, for 30 days. The model takes approximately 30 h to run for the full Midcoast Maine area for 30 days at a 10-day interval. Output grids include shell length, total fresh weight (TFW), dry soft tissue weight, dry condition index, wet condition index, cumulative clearance volume, cumulative nitrogen excretion, cumulative oxygen volume uptake, cumulative total mass deposited as pseudofeces, cumulative total mass deposited as true feces, cumulative total mass deposited as both pseudofeces and true feces, number of animals harvested, and total biomass harvested. Here, only growth predicted as TFW of oysters and mussels over the entire coast of Maine was presented.

The satellite image for July 14, 2013 covers the coastal area from Portland to Thomaston. Unfortunately, there were no coincident data for the eastern coastal area. Although it was 3 y later, the best quality satellite data for the eastern area at a similar time of year were August 23, 2016. The model was also run for this date for the eastern Maine region. Because the Midcoast Maine region has warmer water and is better habitat for *Crassostrea virginica*, here, the results for this species in the July 14 image were presented. The results for the colder, eastern area of Maine for the two species which also grow better in colder waters (*Mytilus edulis* and *Ostrea edulis*) were presented.

ShellGIS produces results that can be visualized and queried with a “point and click” method. The images show areas of red and yellow where TFW has increased from an initial size of 5.2 g, green where there is a slight increase in TFW, and blue where there is a decrease in TFW over the 30-day period. There are artifacts in the images right next to the shoreline and from some clouds. Future work may help to remove these types of artifacts. Clear differences between the eastern and western images are to be expected, given their different dates.

Results are shown for three shellfish species: the blue mussel *Mytilus edulis*, the eastern oyster *Crassostrea virginica*, and the European flat oyster *Ostrea edulis*. Users can click on individual parts of the images to reveal the TFW value for that location. Predicted growth is presented for all three species in Figure 3 (blue mussels, 3A; eastern oysters, 3B; and European flat oysters, 3C). Predictions within these images are consistent with the results of Snyder et al. (2017), including the locations of current commercial shellfish farms in Maine, while also highlighting some promising areas that are not currently under cultivation.

## DISCUSSION

It is generally acknowledged that turbidity and associated inorganic matter may limit oyster growth through the dilution of organic dietary constituents (e.g., Thomas et al. 2011, Snyder et al. 2017, Adams et al. 2019, Palmer et al. 2020). Furthermore, models of bivalve growth that do not explicitly address responsive adjustments in the filtration and absorption of POM may have limited application between

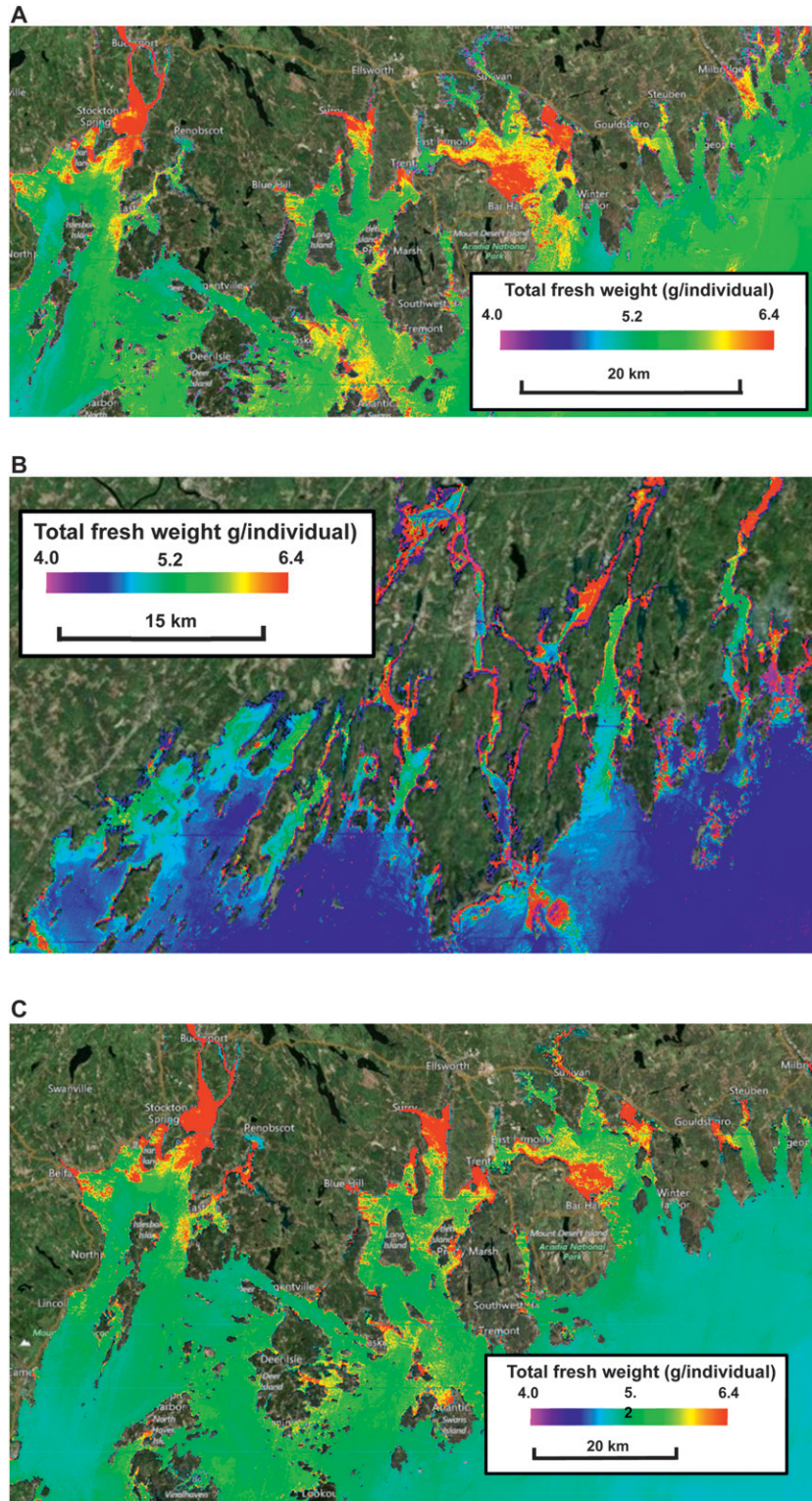


Figure 3. (A) Blue mussel predicted growth in July in eastern Maine in ShellGIS using constant drivers based on satellite images. The images show areas of red and yellow where total fresh weight (TFW) has increased, green where there is a slight increase in TFW, and blue where there is a decrease in TFW over the 30-day period. (B) Eastern oyster predicted growth in July in Midcoast and eastern Maine in ShellGIS using constant drivers based on satellite images. The images show areas of red and yellow where TFW has increased, green where there is a slight increase in TFW, and blue where there is a decrease in TFW over the 30-day period. A different color scheme was used in this image to highlight differences in predicted growth. (C) European flat oyster predicted growth in eastern Maine in ShellGIS using constant drivers based on satellite images. The images show areas of red and yellow where TFW has increased, green where there is a slight increase in TFW, and blue where there is a decrease in TFW over the 30-day period.

contrasting geographical areas across which both the composition and bioavailability of that POM may vary (Pusceddu et al. 1996, Dauwe et al. 1999, Monaco et al. 2019). Instead, simulation of bivalve growth across different habitats has been improved in the ShellSIM growth model by including relations which define dynamic adjustments between the relative ingestion and absorption of both CHL-rich and all remaining organics such as bacteria, protozoans, colloids, and/or detritus, thereby helping to account for changes in seston composition that may vary greatly both in time and space (Hawkins et al. 2013b). Such resolution is likely to be important when using remote sensing to source model drivers over large areas. Described here is a means to predict POM using CHL and turbidity derived from satellite images, over ranges of CHL ( $<28 \mu\text{g L}^{-1}$ ) and SPM ( $<200 \text{mg L}^{-1}$ ) that span most natural environments (Hinga et al. 1995, Gernez et al. 2014, 2017), and throughout which ranges bivalve growth is maintained through interrelated adjustments in feeding and digestion (Hawkins et al. 2013a, 2013b). Such predictions are able to predict oyster growth adequately in Maine and Connecticut (Fig. 1).

Prediction of SPM from optical measurements followed the method of Snyder et al. (2017), where there was a 1/1 relationship between satellite turbidity and turbidity measured *in situ* using a Sea-Bird Water Quality Monitor Backscatter sensor

calibrated with a Hach turbidity meter. A relationship of 1/1 from SPM ( $\text{mg L}^{-1}$ ) to sensor-calibrated turbidity (NTU) was used, but this relationship can depend on particle size and has been shown to vary from 1/1 in the winter to 2/1 in the summer (Jafar-Sidik et al. 2017).

There may be certain environments where the relationship among POM, CHL, and SPM reported in Eq. 1 earlier will not apply, such as in riverine systems where PIM dominates the suspended fraction and POC is as low as 1% of the total suspended matter (Etcheber et al. 2007). In addition, water salinity is not currently measured with remote sensing, but which may be proven correlated with colored dissolved organic matter, thus with potential to further enhance associated predictions of bivalve growth. Regardless, given that detritus often contributes to suspended particulates, the simple predictive equation for POM as presented here represents a convenient means whereby high-resolution satellite images may be used to compare the relative growth of bivalves over large and contrasting regions of the coastal zone. Whereas obtaining time series data from cloud-free satellite images may be challenging, the GIS presentation of the relative growth of multiple bivalve species using a growth model driven by both CHL and POM from a single image provides a useful tool for aquaculture site selection and the restoration of native species.

#### LITERATURE CITED

- Adams, C. M., L. M. Mayer, P. Rawson, D. C. Brady & C. Newell. 2019. Detrital protein contributes to oyster nutrition and growth in the Damariscotta estuary, Maine, USA. *Aquacult. Environ. Interact.* 11:521–536.
- Dauwe, B., J. J. Middelburg, P. M. J. Herman & C. H. R. Heip. 1999. Linking diagenic alteration of amino acids and bulk organic matter reactivity. *Limnol. Oceanogr.* 44:1809–1814.
- Development Team Q.G.I.S. 2012. QGIS geographic information system. Open Source Geospatial Foundation Project. Available at: <http://qgis.org>.
- Etcheber, H., A. Taillez, G. Abril, J. Garnier, P. Servais, F. Moatar & M. V. Commarieu. 2007. Particulate organic carbon in the estuarine turbidity maxima of the Gironde, Loire and Seine estuaries: origin and lability. *Hydrobiologia* 588:245–259.
- Franz, B. A., S. W. Bailey, N. A. Kuring & J. Werdell. 2015. Ocean color measurements with the operational land imager on Landsat-8: implementation and evaluation in SeaDAS. *J. Appl. Remote Sens.* 9:096070.
- Gernez, P., L. Barillé, A. Lerouxel, C. Mazeran, A. Lucas & D. Doxaran. 2014. Remote sensing of suspended particulate matter in turbid oyster-farming ecosystems. *J. Geophys. Res. Oceans* 119: 7277–7294.
- Gernez, P., D. Doxaran & L. Barillé. 2017. Shellfish aquaculture from space: potential of Sentinel2 to monitor tide-driven changes in turbidity, chlorophyll concentration and oyster physiological response at the scale of an oyster farm. *Front. Mar. Sci.* 4:137.
- Hawkins, A. J. S., P. L. Pascoe, H. Parry, M. Brinsley, K. D. Black, C. McGonigle, H. Moore, C. R. Newell, N. O'Boyle, T. O'Carroll, B. O'Loan, M. Service, A. C. Smaal, X. L. Zhang & M. Y. Zhu. 2013a. ShellSIM: a generic model of growth and environmental effects validated across contrasting habitats in bivalve shellfish. *J. Shellfish Res.* 32:237–253.
- Hawkins, A. J. S., P. L. Pascoe, H. Parry, M. Brinsley, F. Cacciatore, K. D. Black, J. G. Fang, H. Jiao, C. McGonigle, H. Moore, N. O'Boyle, T. O'Carroll, B. O'Loan, M. Service, A. C. Small, X. Yan, J. H. Zhang, X. L. Zhang & M. Y. Zhu. 2013b. Comparative feeding on chlorophyll-rich versus remaining organic matter in bivalve shellfish. *J. Shellfish Res.* 32:883–897.
- Hinga, K. R., H. Jeon & N. F. Lewis. 1995. Marine eutrophication review. I: quantifying the effects of nitrogen enrichment on phytoplankton in coastal ecosystems. Silver Spring, MD: NOAA Coastal Ocean Office. 36 pp.
- Jafar-Sidik, M., F. Gohin, D. Bowers, J. Howarth & T. Hull. 2017. The relationship between suspended particulate matter and turbidity at a mooring station in a coastal environment: consequences for satellite-derived products. *Oceanologia* 59:365–378.
- Legendre, L. & J. Michaud. 1999. Chlorophyll a to estimate the particulate organic carbon available as food to large zooplankton in the euphotic zone of oceans. *J. Plankton Res.* 21:2067–2083.
- Monaco, C. J., E. M. Porporato, J. A. Lathlean, M. Tagliarolo, G. Sarà & C. D. McQuaid. 2019. Predicting the performance of cosmopolitan species: dynamic energy budget model skill drops across large spatial scales. *Mar. Biol.* 166:14.
- Newell, C. R., A. J. S. Hawkins, K. Morris, J. Richardson, C. Davis & T. Getchis. 2013. ShellGIS: a dynamic tool for shellfish farm site selection. *World Aquac.* 44:50–53.
- Palmer, S. C., P. M. Gernez, Y. Thomas, S. Simis, P. I. Miller, P. Glize & L. Barillé. 2020. Remote sensing-driven Pacific oyster (*Crassostrea gigas*) growth modeling to inform offshore aquaculture site selection. *Front. Mar. Sci.* 6:802.
- Pusceddu, A., E. Serra, O. Sanna & M. Fabiano. 1996. Seasonal fluctuations in the nutritional value of particulate organic matter in a lagoon. *Chem. Ecol.* 13:21–37.
- Radiarta, I. N., S. I. Saitoh & A. Miyazono. 2008. GIS-based multi-criteria evaluation models for identifying suitable sites for Japanese scallop (*Mizuhopecten yessoensis*) aquaculture in Funika Bay, southwestern Hokkaido, Japan. *Aquaculture* 284:127–135.
- Snyder, J., E. Boss, R. Weatherbee, A. C. Thomas, D. Brady & C. Newell. 2017. Oyster aquaculture site selection using Landsat

- 8-derived sea surface temperature, turbidity, and chlorophyll a. *Front. Mar. Sci.* 4:190.
- Thomas, A. C., D. Byrne & R. Weatherbee. 2002. Coastal sea surface temperature variability from LANDSAT infrared data. *Remote Sens. Environ.* 81:262–272.
- Thomas, Y., J. Mazurié, M. Alunno-Bruscia, C. Bacher, J. F. Bouget, F. Gohin, S. Pouvreau & C. Struski. 2011. Modelling spatio-temporal variability of *Mytilus edulis* (L.) growth by forcing a dynamic energy budget model with satellite-derived environmental data. *J. Sea Res.* 66:308–317.
- Wang, G., W. Zhou, W. Cao, J. Yin, Y. Yang, Z. Sun, Y. Zhang & J. Zhao. 2011. Variation of particulate organic carbon and its relationship with bio-optical properties during a phytoplankton bloom in the Pearl River estuary. *Mar. Pollut. Bull.* 62: 1939–1947.
- Woźniak, S. B., M. Darecki, M. Zabocka, D. Burska & J. Dera. 2016. New simple statistical formulas for estimating surface concentrations of suspended particulate matter (SPM) and particulate organic carbon (POC) from remote-sensing reflectance in the southern Baltic Sea. *Oceanologia* 58:161–175.